Interplay between the vortex phase coherence and extended disorder defects in the vortex-liquid regime of thin films and superlattices of 123 superconductors

E. M. González,[1,*] J. M. González,[2] and J. L. Vicent[1]
[1]*Departamento Física de Materiales, F. Físicas, Universidad Complutense, 28040 Madrid, Spain*
[2]*Departamento Propiedades Opticas, Magnéticas y de Transporte, Instituto de Ciencia de Materiales de Madrid (CSIC), 28049 Cantoblanco (Madrid), Spain*
(Received 23 June 2000)

a-axis oriented (CuO_2 planes perpendicular to the substrate) films and superlattices grown on cubic substrates show a structure with 90° microdomains. The microdomains are grains with a 90° rotation of the *c* axis. In the vortex liquid region, this microstructure induces a change from the usual three-dimensional (3D) behavior of the anisotropy toward a 2D behavior, in a temperature range above the usual crossover from 2D to 3D. Moreover, when the thickness of the superconducting part of the multilayers becomes smaller (or of the same order as) than the microdomain size the 3D dimensional anisotropy behavior is recovered.

A real vortex matter could be studied in high-temperature superconductors (HTS's) with a rich variety and still not well understood vortex phases.[1] The associated phenomenology (vortex glass, Bose glass, splayed glass, vortex liquid, melting, lock-in transition, and so on) reflects a complex interplay among the structural anisotropy, disorder, and small coherence lengths. The high temperature at which the vortex matter can be studied is crucial to that phenomenology.

Recently, several authors have reported the effects of different types of defects on the vortex liquid behavior in single crystals[2] and melt textured[3] 123 cuprates. Lopez *et al.*[2] found strongly entangled vortex liquid in single crystals governed by pointlike disorder; Puig *et al.*[3] found that random quenched and correlated disorders compete in the liquid phase of melt textured $YBa_2Cu_3O_7$ composites.

In this paper we focus on the effect of the interplay between extended disorder defects and the vortex phase coherence lengths in the anisotropy and dimensionality of thin films in the vortex liquid regime. We report anisotropy effects in the liquid vortex phase of the 123 superconducting cuprates. In general, dimensionality and anisotropy problems are ruled by the interplay between different length scales which govern the physics of the problem. Therefore, the experimental length scale (for instance, the relevant sample size) should be comparable to relevant physics length scale (for instance, vortex length). The behavior reported in this work is due to the competition between the microstructural defects and vortex lengths. This interplay leads to a strong deviation from the typical 3D behavior of the anisotropy close to T_c.[1,4] The usual 3D anisotropy behavior is only recovered when artificial HTS superlattices of the adequate modulation lengths are fabricated.

The samples used in this work were the so-called *a*-axis oriented films and superlattices.[5] In these samples, the superconducting CuO_2 planes are grown perpendicular to the substrate. The samples are *a*-axis $EuBa_2Cu_3O_7$ films and *a*-axis $EuBa_2Cu_3O_7/PrBa_2Cu_3O_7$ multilayers. They have been obtained by dc magnetron sputtering in the on-axis configuration on cubic (100) $SrTiO_3$ substrates and their structural and transport characterization have been reported elsewhere.[6] The most relevant structural characteristic of *a*-axis films, grown on cubic substrates, is a microstructure with microdomains of average size around 20 nm with 90° boundaries.[7] Therefore, some experimental care has to be taken with the geometry of the experiment. We have followed a similar experimental geometry that Triscone *et al.*[8] The films were patterned with bridges making a 45° angle with the direction of the CuO_2 planes, and, in our case, the macroscopic current and the magnetic fields are perpendicular to each other (constant Lorentz force configuration). A simple correction has to be used in the anisotropy expressions to relate the value of the angle θ between the film normal and the applied magnetic field H and the angle φ, between H and the CuO_2 planes, see Vélez *et al.*[6] It is worthwhile to stress that high-resolution-transmission electron microscopy in our *a*-axis films and superlattices have shown the typical 90° microdomains,[9] and that in the case of the superlattices, refinement of the structure from x-ray spectra shows that the interface step disorder is around 1 unit cell and the interface diffusion is 20 percent,[10] values very similar to the values obtained in *c*-axis superlattices.[11]

We have to point out that, in-plane-aligned *a*-axis films have been fabricated[12] on tetragonal substrates ($LaSrGaO_4$). In this case, the microdomain structure is, of course, absent, only antiphase boundaries and stacking faults have been observed.[13]

The anisotropy of the samples were studied using a commercial 90 kOe superconducting magnet, standard resistivity dc technique and a computer controlled rotatable sample holder. The value $\theta = 0°$ is with the applied magnetic field perpendicular to the film plane, that is parallel to the CuO_2 planes direction. The raw data we have used to analyze the anisotropic behavior are taken with a constant current density of 80 A/cm^2, close to T_c, in the vortex liquid regime. Variation of the current density around this value and the temperature above 0.85 T/T_c do not change the results. Figure 1 shows that the applied magnetic fields and current density used in the experiment explore this vortex liquid region. These (ρ, J) curves are extracted from current-voltage (I, V) characteristics, with the applied magnetic field perpendicular

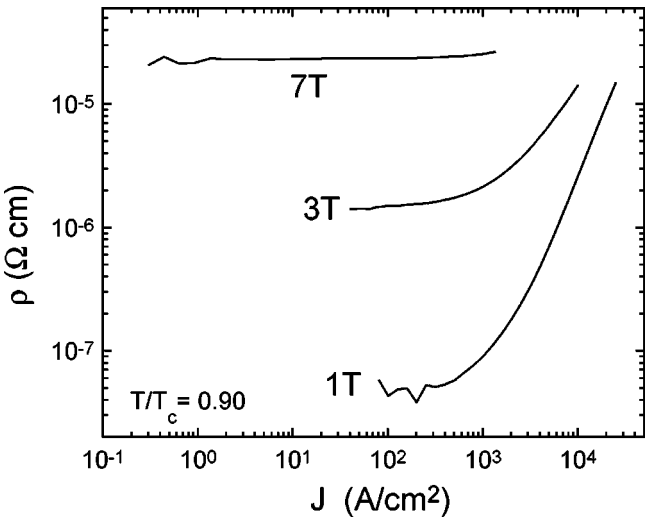

FIG. 1. Resistivity vs the current density, in a double logarithmic scale, for an *a*-axis $EuBa_2Cu_3O_7$ film at $T/T_c=0.9$. The magnetic field is perpendicular to the film plane. This figure shows that the magnetic fields and currents used in the measurements correspond to the linear behavior of the vortices in the liquid phase.

to the substrate (parallel to the CuO_2 planes). Figure 2 shows $[\rho(\theta),\mathrm{H}_i]$ curves, that is, resistivity vs θ (angle between the applied magnetic field and the normal to the film) at the constant field H_i. From these sets of measurements we easily extract the $[\rho(H_i),\theta_j]$ curves: at fixed angles θ_j (ranging from 0° to 90°), the ρ value at every measured field H_i is taken. This last set of curves is used in our analysis later.

Among the HTS families, the 123 cuprates are one of the less anisotropic, following a 3D behavior close to T_c.[1] Therefore the 3D effective-mass model is a good starting point to analyze the data. In the framework of this model, one step further is given by Lawrence and Doniach.[14] This approach opens the possibility of a dimensional crossover decreasing the temperature. A clear hint of a crossover from a 3D to a 2D behavior was experimentaly observed in intrinsic[15] and artificial[16] low-temperature superconducting

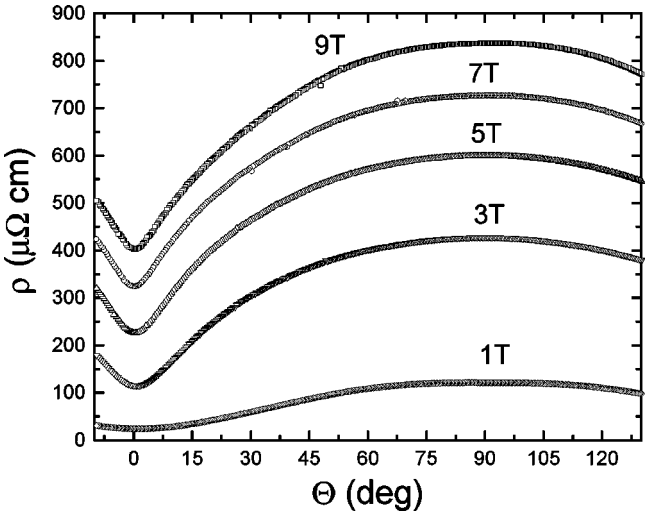

FIG. 2. Raw data at $T/T_c=0.9$ for an *a*-axis $EuBa_2Cu_3O_7$ film showing the resistivity vs the angle θ at several constant fields. The measurement current density was 80 A/cm^2.

superlattices. The *L-D* model, which comes from the Ginzburg-Landau equations, investigates layered superconducting systems with the superconducting order parameter, in adjacent layers, coupled by Josephson tunneling. In this case, a loss of the coherence of the order parameter phase occurs, and the usual HTS picture of pancake vortices and Josephson vortices could come up easily.[1] For these reasons, the *L-D* approach seems to be a perfect tool to study problems of anisotropy and dimensionality in HTS. Unfortunately, the upper critical field H_{c2} is the experimental quantity that is calculated. The use of the scaling approach, proposed by Blatter *et al.*,[17] helps to solve this problem. This approach allows us to translate various superconducting properties from isotropic to anisotropic systems. In particular, the magnetic field at any angle is scaled to a reduced field as $H_{\mathrm{red}}=H\epsilon(\varphi)$, where the factor $\epsilon(\varphi)$ comes from the anisotropy models according to the definition $\epsilon(\varphi)=H_{c2}(\varphi)/H_{c2}^{\parallel}$ (φ: angle between H and Cu-O planes, $H_{c2}^{\parallel}$: upper critical field parallel to the Cu-O planes). Several authors have used this approach to avoid the H_{c2} problem and to study anisotropy and dimensionality in HTS (see, for instance, Ref. 18). The scaling function, used in the definition of the reduced field in the 3D model, is given by $\epsilon(\varphi)=\sqrt{\sin^2\varphi+\gamma^2\cos^2\varphi}$; where the anisotropy parameter is defined as $\gamma=H_{c2}^{\perp}/H_{c2}^{\parallel}$ and $H_{c2}^{\perp}$ is the upper critical field perpendicular to the CuO_2 planes. As was pointed out (see Ref. 6), the measurement configuration let φ be expressed as a function of the angle θ according to $\sin\varphi=\sin\theta\sin\phi$ (in our case, $\phi=45°$). Therefore, taking into account this last relation, the anisotropy factor ϵ can be written as a function of the angle θ, $\epsilon=\epsilon(\theta)$, so this is the expression that we use in the graphs.

A scaling rule given by $H\mapsto Hf(\theta)$ (f is a factor that only depends on the angle) applies successfully in these *a*-axis oriented films for sets of resistivity measurements $[\rho(H_i),\theta_j]$, see Fig. 3(a). In these collapses, the *f* factors are not extracted from any anisotropy model. The comparison with the models is presented in Fig. 3(b), where the ϵ/γ values vs θ are plotted. The same behavior has been observed at other temperatures above $T/T_c=0.85$, also. These plots show a clear deviation of the 3D behavior. First of all, this means that the anisotropy in *a*-axis $EuBa_2Cu_3O_7$ films on cubic (100) $SrTiO_3$ substrates does not follow the 3D anisotropy behavior of H_{c2}. However, we were able to fit the experimental data [see Fig. 3(b)] around the CuO_2 planes direction (0°–20°) using the Yamafuji *et al.* model[19] (YKI). In this model, $H_{c2}(\varphi)$ is calculated by applying a perturbation method to the Ginzburg-Landau equation. The final expression is

$$\frac{H_{c2}(\varphi)}{H_{c2}^{\perp}}\sin(\varphi)+\left(\frac{H_{c2}(\varphi)}{H_{c2}^{\parallel}}\cos(\varphi)\right)^2 \times\left[1-3(1+\sqrt{2})\left(\frac{H_{c2}^{\perp}}{H_{c2}^{\parallel}}\right)^2\frac{H_{c2}(\varphi)}{H_{c2}^{\perp}}\sin(\varphi)\right]=1.$$

Actually, the YKI model is a further step in the Tinkham model,[20] that explores the behavior of H_{c2} in superconducting thin films.

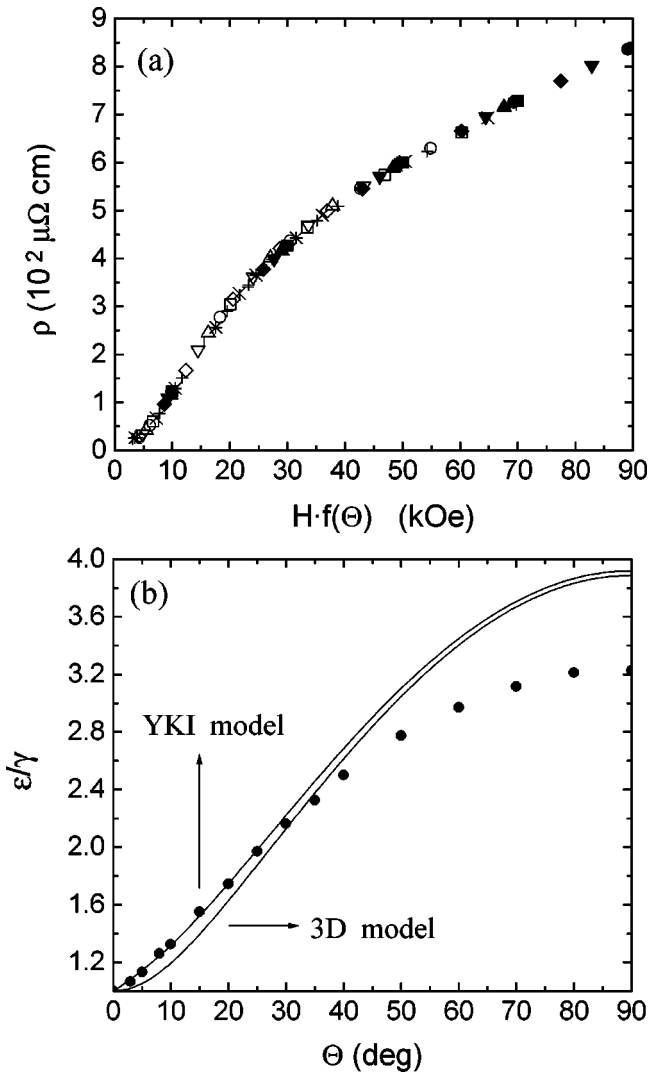

FIG. 3. a-axis $EuBa_2Cu_3O_7$ oriented film (thickness 250 nm) at $T/T_c=0.90$. (a) Resistivity vs the reduced field variable $Hf(\theta)$ showing the collapse of the experimental $\rho(H)$ curves at angles θ: 0°, 3°, 5°, 8°, 10°, 15°, 20°, 25°, 30°, 35°, 40°, 50°, 60°, 70°, 80°, and 90°. (b) Experimental points of ϵ/γ, extracted from Fig. 3(a), vs the θ angle (see text). The predicted angular dependence of the anisotropy models are also plotted for comparison. The anisotropy parameter is $\gamma=0.185$.

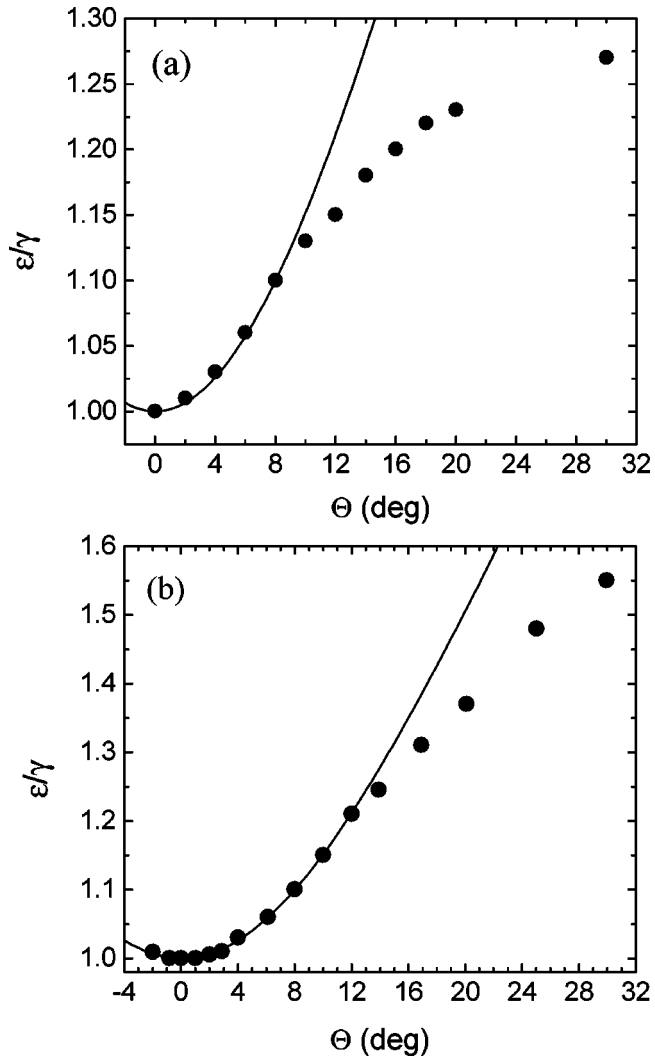

FIG. 4. Experimental points of ϵ/γ vs θ angle for two different superlattices (total thickness 250 nm) at the same reduced temperature $T/T_c=0.90$. The solid line is the prediction of the 3D model. (a) Superlattice of bilayer 50 u.c. $EuBa_2Cu_3O_7$/5 u.c. $PrBa_2Cu_3O_7$ (u.c. means unit cells). (b) Superlattice of bilayer 25 u.c. $EuBa_2Cu_3O_7$/5 u.c. $PrBa_2Cu_3O_7$.

Before we begin to analyze these results, it is worthwhile to note that recently, Trajanovic *et al.*[21] have studied the anisotropy and dimensionality effects in untwinned in-plane-aligned a-axis $YBa_2Cu_3O_7$ films, at a lower temperature range than in our case. These authors could fit the data simply by replacing H_{c2} with J_c in the anisotropy models. They found that the critical current J_c follows the $H_{c2}(\varphi)$ anisotropy laws in the whole (0°–90°) angular interval, with a 3D behavior at high temperatures and a crossover, as expected, to 2D (Tinkham thin-film model) decreasing the temperature below $T/T_c=0.8$. However, this expected 3D behavior is absent in our a-axis films with 90° microdomains. In our case, the experimental data could only be fitted to a model (YKI), related to the Tinkham model, in an angular region around the CuO_2 superconducting planes.

Anisotropy and dimensionality effects are only a matter of comparison between different length scales. Thereby, the different lengths involved in the problem have to be discussed. One of them related to the sample characteristics and the other to the superconducting properties.

The microdomains are the unique structural difference between the in-plane-aligned films (3D anisotropy) and our samples (deviation from the expected 3D anisotropy). The sample characteristic length could be related to the peculiar film microstructure (20 nm average size microdomains with 90° boundaries). The superconducting characteristic length must be at least of the same order to have the possibility of a dimensional crossover. The experimental window could be a clue to clarify this point. The measurements are taken at temperatures above 0.85 T/T_c and with applied magnetic field of the order of 50 kOe. Taking into account that the intervortex distance a_0 is given by $a_0=1.07\ (\Phi_0/B)^{1/2}$, where Φ_0 is the fluxoid, the intervortex distance is of the order of the microdomain size, and, besides, the temperatures are close to T_c, so the vortices are very soft. The next step should be to discuss the influence of the microstructure in the

entanglement regime. But, before that, we have to clarify which vortex length is ruling this effect. In the 3D case the vortex is well defined along the sample and the flux jumps do not implicate that the vortex loses its identity. In our case, the dimensionality could be reduced if the vortex phase coherence is lost. The vortex length that should be taken into account is related to the phase correlation of the superconducting order parameter in the direction of the applied magnetic field. That is, the length along the vortex where it exists as a phase coherent object. The superconducting length which matters is the vortex phase correlation. When the vortex phase correlation is lost, cutting and recombination of vortices take place.[22] The dimensionality and anisotropy picture follows, in our case, from the competition of two lengths: the size of the microdomains and the vortex coherence length. At each angle, the phase coherence length would be given by the vortex length within a microdomain; when that length gets shorter than some other reference length, such as the natural phase coherence length due to vortex entanglement, then the angular dependence could be strongly affected. We assume that the microstructure and its 90° boundaries could act as barriers cutting and reconnecting vortex lines. These films do show vortex cutting induced by correlated disorder. This behavior deviates from the role plays by extended correlated disorder (twin boundaries, columnar defects) which induces vortex correlation for fields parallel to extended defects.[22]

How do we test this assumption without changing the temperature (combing the vortices) and the structure of the material? Superconducting multilayers are the ideal tool to do it. The key could be multilayers with superconducting layer thicknesses of the order or smaller than the microdomain size. Figure 4(a) shows the dimensional behavior of *a*-axis $EuBa_2Cu_3O_7/PrBa_2Cu_3O_7$ (50/5 u.c.) superlattice grown on cubic (100) $SrTiO_3$ substrates. This sample follows a 3D effective mass model behavior when the magnetic field is applied close to the CuO_2 planes, with an anisotropy parameter, γ, typical of the 123 cuprates.[1] In this multilayer, the thickness of the superconducting layers and the size of the microdomains are of the same order. If the thickness of the superconducting layer is reduced even more (25 u.c.), see Figure 4(b), the experimental data follows the 3D model in a broader angular interval than before. In summary, when the magnetic field is applied close to the CuO_2 planes and the superconducting layer thickness (vortex length) is of the order or smaller than the microdomain size, the system follows the usual 3D anisotropy model. But, when the microdomain size is smaller than the vortex length, the 90° boundaries could be seen by the vortices and cutting and recombination could occur. Then, a deviation of the typical 3D behavior happens. Finally, it has to be noted that in these *a*-axis superlattices the superconducting layers are not decoupled; the PBCO layer thickness is only 2 nm, much smaller than the decoupling length estimated by Suzuki *et al.*[23] The superlattices are in the strong coupling regime, the microdomain boundaries are the main actors in this crossover effect.

In conclusion, in the vortex liquid regime, the anisotropy of *a*-axis films grown on cubic substrates follows the $H_{c2}(\theta)$ behavior given by the YKI model when the magnetic field is applied between 0° (parallel to the CuO_2 planes) and 20°. This behavior is due to the change of the vortex phase coherence length, which is modified by the microstructure of the film. The 90° microdomains induce correlated disorder cutting and recombination of the vortices. The expected 3D anisotropy behavior is only observed when superlattices of the appropiate modulation length are fabricated.

The authors want to thank I. K. Schuller, F. de la Cruz and G. Crabtree for useful conversations. This work has been supported by Spanish CICYT (MAT99-724).

*Present address: Department of Physics, SUNY, Stony Brook, NY 11794.

[1] G. Blatter *et al.*, Rev. Mod. Phys. **66**, 1125 (1994); J.M. Triscone and O. Fisher, Rep. Prog. Phys. **60**, 1673 (1997); I. Bozovic and J. N. Eckstein, *Physical Properties of High Temperatures Superconductors V*, edited by D.M. Ginsberg (World Scientific, Singapore, 1996), p. 99.
[2] D. Lopez *et al.*, Phys. Rev. Lett. **80**, 1070 (1998).
[3] T. Puig *et al.*, Phys. Rev. B **60**, 13 099 (1999); T. Puig and X. Obradors, Phys. Rev. Lett. **84**, 1070 (2000).
[4] C.S.L. Chun *et al.*, Phys. Rev. B **29**, 4915 (1984).
[5] C.B. Eom *et al.*, Science **251**, 780 (1991).
[6] M. Vélez *et al.*, Phys. Rev. B **54**, 101 (1996), and references therein.
[7] C.B. Eom *et al.*, Science **249**, 1549 (1990); A.F. Marshall and C.B. Eom, Physica C **207**, 239 (1993).
[8] J.-M. Triscone *et al.*, J. Alloys Compd. **183**, 224 (1992).
[9] J.I. Martin *et al.*, Thin Solid Films **275**, 119 (1996).
[10] E.M. Gonzalez *et al.*, *Stripes and Related Phenomena*, edited by A. Bianconi and N.L. Saini (Kluwer Academic/Plenum Publishers, New York, 2000), p. 539.
[11] E.E. Fullerton *et al.*, Phys. Rev. Lett. **69**, 2859 (1992).
[12] K.H. Young and J.Z. Sun, Appl. Phys. Lett. **59**, 2448 (1991).
[13] Y. Suzuki *et al.*, Phys. Rev. B **48**, R10 642 (1993).
[14] W.E. Lawrence and S. Doniach, *Proceedings of the 12th International Conference on Low Temperature Physics*, edited by E. Kanda (Academic Press, Kyoto, 1971), p. 361.
[15] J.L. Vicent *et al.*, Phys. Rev. Lett. **44**, 892 (1980).
[16] S.T. Ruggiero *et al.*, Phys. Rev. Lett. **45**, 1299 (1980).
[17] G. Blatter *et al.*, Phys. Rev. Lett. **68**, 875 (1992).
[18] E. Silva *et al.*, Phys. Rev. B **55**, 11 115 (1997); H. Iwasaki *et al.*, Physica C **244**, 71 (1995); C.M. Fu *et al.*, *ibid.* **205**, 111 (1993).
[19] K. Yamafuji *et al.*, Phys. Lett. **20**, 122 (1966).
[20] M. Tinkham, Phys. Lett. **9**, 217 (1964).
[21] Z. Trajanovic *et al.*, Phys. Rev. B **56**, 925 (1997).
[22] D. Lopez *et al.*, Phys. Rev. Lett. **76**, 4034 (1996).
[23] Y. Suzuki *et al.*, Phys. Rev. Lett. **73**, 328 (1994).